JACS
JOURNAL OF THE AMERICAN CHEMICAL SOCIETY
Communication
pubs.acs.org/JACS

A Single-Component Molecular Superconductor

HengBo Cui,[†] Hayao Kobayashi,*[,∥] Shoji Ishibashi,[§] Masaaki Sasa,[‡] Fumitatsu Iwase,[†] Reizo Kato,[†] and Akiko Kobayashi*[,∥]

[†]Condensed Molecular Materials Laboratory, RIKEN, Wako-shi, Saitama 351-0198, Japan

[∥]Department of Chemistry, College of Humanities and Sciences, Nihon University, Sakurajosui, Setagaya-ku, Tokyo 156-8550, Japan

[§]Nanosystem Research Institute (NRI) "Research Initiative of Computational Sciences (RICS)", National Institute of Advanced Industrial Science and Technology (AIST), 1-1-1 Umezono, Tsukuba, Ibaraki 305-8568, Japan

[‡]R&D Strategy and Planning Office, FUJITSU R&D CENTER CO., LTD, 13/F, Tower A, Ocean International Center, NO.56 Dong Si Huan Zhong Rd, Chaoyang District, Beijing P. R. China 100025

Supporting Information

ABSTRACT: The pressure dependence of the resistivities of a single-component molecular conductor, $[Ni(hfdt)_2]$ (hfdt = bis(trifluoromethyl)tetrathiafulvalenedithiolate) with semiconducting properties at ambient pressure was examined. The four-probe resistivity measurements were performed up to ~10 GPa using a diamond anvil cell. The low-temperature insulating phase was suppressed above 7.5 GPa and the resistivity dropped, indicating the superconducting transition occurred around 7.5−8.7 GPa with a maximum T_c (onset temperature) of 5.5 K. The high-pressure crystal and electronic band structures were derived by the first-principle calculations at 6−11 GPa. The crystal was found to retain the semiconducting band structure up to 6 GPa. But the electron and hole Fermi surfaces appear at 8 GPa. These results of the calculations agree well with the observation that the pressure-induced superconducting phase of $[Ni(hfdt)_2]$ appeared just above the critical pressure where the low-temperature insulating phase was suppressed.

The single-component molecular superconductor is considered to be one of the ultimate goals in the search for new molecular materials with unprecedented electronic properties. The first organic superconductor composed of organic π-donors and inorganic mono-anions, $(TMTSF)_2PF_6$ (TMTSF = tetramethyltetraselenafulvalene), was reported 34 years ago, and the first molecular superconductor, whose main component was a transition metal dithiolate complex, i.e., $(TTF)[Ni(dmit)_2]_2$ (TTF = tetrathiafulvalene; dmit =1,3-dithiol-2-thione-4,5-dithiolate) was discovered 28 years ago.[1,2] Since then, many molecular superconductors have been reported. However, all these molecular superconductors were composed of more than two chemical species, and most of chemists considered the single-component molecular crystals to be insulators until the beginning of this century,[3,4] although the superconducting transitions were observed in iodanil and hexaiodobenzene under extremely high pressures.[5]

In 1996, Underhill et al. and Bijϕrnholm et al. developed the conducting single-component molecular crystals composed of nickel and gold complexes with dithiolate ligands, $[Ni(MeS_2dt)_2]$ (MeS_2dt = dimethylthiotetrathiafulvalenedithiolate; $\sigma(RT) \sim 10^{-1}$ S cm^{-1}) and $[Au(bdt)_2]$ (bdt = bis(benzene-1,2-dithiolato); $\sigma(RT) \sim 8 \times 10^{-3}$ S cm^{-1} at 0.54 GPa), respectively (Figure 1).[6] In 2001, we prepared a single crystal

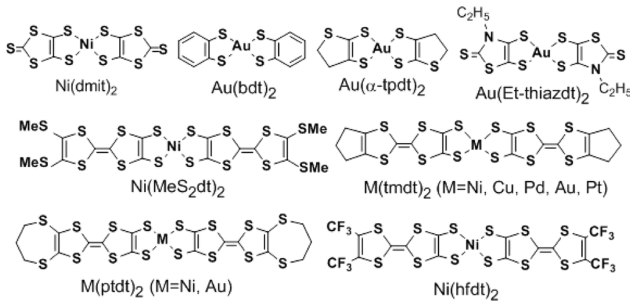

Figure 1. Molecules and the abbreviations.

of $[Ni(tmdt)_2]$ (tmdt = trimethylenetetrathiafulvalenedithiolate) with room-temperature conductivity of ~400 S cm^{-1} and observed metallic behavior down to very low temperatures.[7] Around the same time, the metallic properties of a single-component molecular crystal $[Au(\alpha\text{-tpdt})_2]$ (α-tpdt =2,3-thiophenedithiolate) were also reported.[8] The electron and hole Fermi surfaces of $[Ni(tmdt)_2]$ were also suggested by ab initio band structure calculations.[9] Furthermore, we observed de Haas-van Alphen oscillations of a tiny single crystal of $[Ni(tmdt)_2]$ using a microcantilever of an atomic force microscope (AFM) and the hybrid magnet at the National High Magnetic Field Laboratory at Florida, which proved strictly the existence of the single-component molecular crystal with 3D Fermi surfaces.[10]

Besides the single-component molecular conductors with normal metallic properties down to very low temperature, the systems exhibiting the antiferromagnetic phase transitions at the temperatures much higher than those of the representative organic superconductors such as $(TMTSF)_2X$ and κ-ET_2X (ET = bis(ethylenedithio)tetrathiafulvalene; X = inorganic mono-anion)[11,12] were also discovered (e.g., $T_N \approx 110$ K for $[Au(tmdt)_2]$ and 95 K for $[Cu(dmdt)_2]$ (dmdt = dimethyltetrathiafulvalenedithiolate).[13,14] Considering that the antiferro-

Received: April 13, 2014
Published: May 9, 2014

   dx.doi.org/10.1021/ja503690m | J. Am. Chem. Soc. 2014, 136, 7619−7622

magnetic and superconducting phases frequently adjacent to each other in the phase diagrams of many superconductors including the organic superconductors, the single-component molecular conductors might be good candidates in the research for a new type of molecular superconductor with higher T_c. The electrical and magnetic properties of a series of isostructural $[M(tmdt)_2]$ (M = Ni, Pt, Cu, Au) systems were examined, and their highly conducting properties down to low temperatures were revealed.[3,7,13,15−19] However, the superconducting transition was not observed to date. The resistivity of the single-component molecular conductor $[Ni(ptdt)_2]$ (ptdt = propylenedithiotetrathiafulvalenedithiolate) with semiconducting properties at ambient pressure was examined up to very high pressures.[20,21] Although the metallization of $[Ni(ptdt)_2]$ was observed around 20 GPa, the superconducting transition was not detected. Pressure-induced metallization was also found in crystals of dithiolate gold complex, $[Au(Et\text{-}thiazdt)_2]$ (Et-thiazdt = *N*-ethyl-1,3-thiazoline-2-thione-4,5-dithiolate and the Se-containing analogous system and also in the crystal of nickel complex, $[Ni(dmit)_2]$.[22] It should be also mentioned that besides the crystals of transition-metal dithiolate complexes, Oakley et al. recently reported the metallization of the insulating crystal of radical dimer molecules $(C_6N_3S_2Se_2H_4)_2$.[23] About a decade ago, we synthesized transition-metal complexes with extended TTF ligands and hexafluoro moieties, (hfdt = bis(trifluoromethyl)tetrathiafulvalenedithiolate), to improve the solubility of the crystals in organic solvents.[24,25] As expected, we obtained single crystals of $[M(hfdt)_2]$ (M = Ni, Au) that exhibited semiconducting properties. Recently, we examined the resistivity of $[Ni(hfdt)_2]$ up to ∼10 GPa using a diamond anvil cell (DAC).

Black plate crystals of $[Ni(hfdt)_2]$ were grown electrochemically, following the reported procedure.[24] The room-temperature structure, electronic band structure, and electrical, magnetic and optical properties were previously reported.[24] To evaluate the possibility of a structural phase transition at a low temperature, the crystal structure was determined at 12, 100, 200, and 250 K but no structure change was detected. Because the crystal belongs to the triclinic system with the space group of *P*-1 (no. 2) and $Z = 1$, all the Ni atoms are on the lattice points. Owing to the strong segregation tendency of the molecules with bulky terminal fluorinated groups,[26] the molecules arranged to form two-dimensional (2D) layers parallel to the *ac*-plane (Figure 2a). The shortest intermolecular F···F distance (e.g., 2.89 Å at 12 K) was much longer than the corresponding van der Waals contact (2.70 Å) even at low temperature. The lattice constants decreased with temperature down to 12 K. The largest thermal contraction was observed along the *b* direction, which was consistent with the 2D character of the structure: $\Delta a = 0.093$ Å, $\Delta b = 0.332$ Å, and $\Delta c = 0.126$ Å between 12 and 295 K (Figure 2b). The average thermal expansion coefficient $((\Delta V/\Delta T)/V)$ was 1.9×10^{-4}/K. As mentioned later, the crystal and electronic band structures were derived by the first-principle calculations at 6−11 GPa. The pressure dependences of the calculated lattice constants are presented in Figure 2c. The large compressibility along the *b* axis is consistent with the 2D nature of the crystal. At 6 GPa, $-\Delta V/V$(at 1 bar) ≈ 0.16. That is, the volume compressibility is roughly estimated as 2.6×10^{-3} kbar^{-1}. The semiconducting electronic band structure at ambient pressure was 2D.[24] A similar 2D but metallic band structure was suggested in $[Au(ptdt)_2]$, which will be due to the relatively small terminal group of $[Au(ptdt)_2]$.[27]

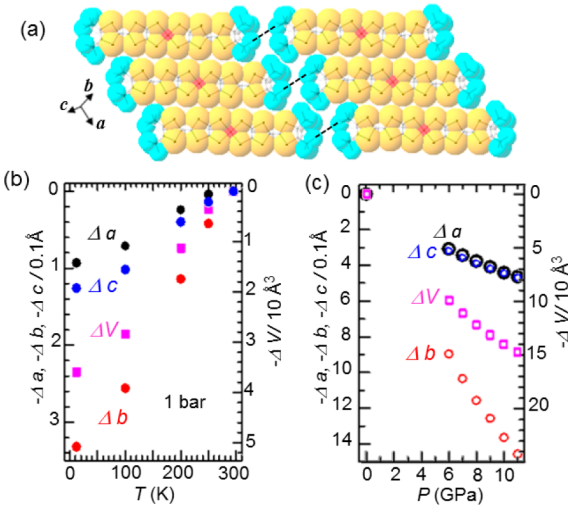

Figure 2. (a) Molecular packing in $[Ni(hfdt)_2]$. The dotted line indicates the shortest intermolecular F···F contact (2.89 Å at 12 K) between the conduction layers parallel to the *ac* plane. (b) Temperature changes of the lattice constants, Δa, Δb, Δc and ΔV: $a = 7.964$, $b = 16.701$, $c = 5.061$ Å, and $V = 665.2$ Å^3 at 295 K.[24] (c) The pressure changes of the lattice constants, *a*, *b*, *c*, and *V* obtained by the first-principle calculations. The large black and small blue open circles and red open circles represent Δa, Δc, and Δb, respectively.

Four-probe resistivity measurements were performed up to ∼10 GPa using a DAC (Figure 3). Crystals with a maximum size of ∼0.12−0.13 mm were used. High-pressure experiments were performed following the reported procedure.[21] Four 10 μm gold wires were attached to the crystal with gold paint and

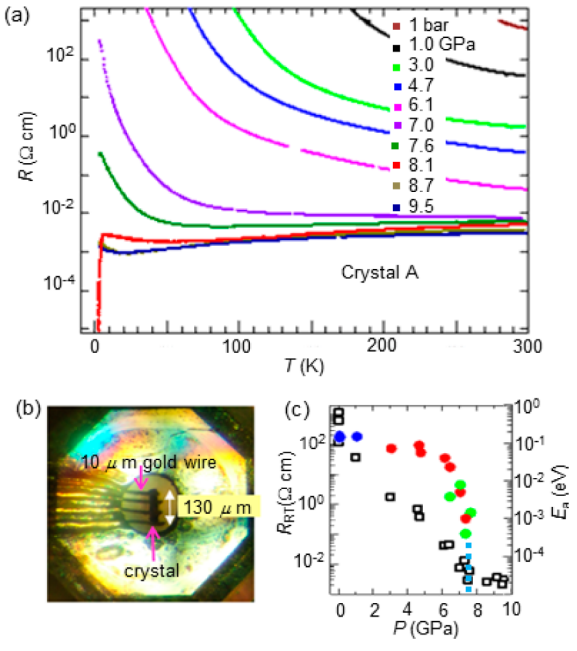

Figure 3. (a) The temperature dependences of the resistivities of $[Ni(hfdt)_2]$ up to ∼10 GPa (crystal A). The resistivities at 1 bar are the data obtained for other crystal (crystal D). (b) A picture of a sample in a DAC. The sample size was $0.13 \times 0.02 \times 0.01$ mm^3. (c) Pressure dependences of the room-temperature resistivity (R_{RT}) (open squares) and the activation energies (E_a) of the resistivities: blue, red, and green circles represent E_a determined at the temperature regions of 300−200 K and around 150 and 10 K, respectively.

dx.doi.org/10.1021/ja503690m | J. Am. Chem. Soc. 2014, 136, 7619−7622

used as leads (Figure 3b). The diamond anvil had a top surface diameter of 0.70 mm, and stainless steel SUS301 was used as the metal gasket. Daphne oil 7373 was used for the pressure medium, and the pressure was determined at room temperature by monitoring the shift of the ruby fluorescence R1 lines.

At ambient pressure, the resistivity showed semiconducting behavior with a room-temperature resistivity of ~6×10^2 Ω cm and an activation energy (E_a) of 0.14 eV (Figure 3a,c).[24] The room-temperature resistivity decreased rapidly with increasing pressure (P) at P < 7 GPa (Figure 3c), but the pressure dependence of E_a was rather sluggish at P < 6 GPa. Around 7.3 GPa, E_a decreased very sharply, and the metallic state appeared above 7.5 GPa. Above 7.3 GPa, the pressure dependence of the room-temperature resistivity became very small (~3×10^{-3} Ω cm). As shown in Figure 3a, at 7.6 GPa, the resistivity gradually decreased down to ~85 K, then increased fairly rapidly with decreasing temperatures, and a very small resistivity decrease was detected around the lowest experimental temperature (~3.3 K) (see Supporting Information (SI)). A sharp resistivity drop indicating the superconducting transition was observed around 8.1 GPa. The onset temperature of the superconducting transition was ~5.5 K. This resistivity behavior clearly indicates the existence of a single-component molecular superconductor. Above 8.7 GPa, a superconducting transition was not observed at least above 3.3 K. As shown in Figure 3a, a slight resistivity increase was observed at low temperatures (8.7 and 9.5 GPa). However, this resistivity increase is not considered an intrinsic property of the system because it was not observed in crystal C (see SI).

The magnetic field dependence of the resistivity was measured up to 7 T. As shown in Figure 4a, the resistivity

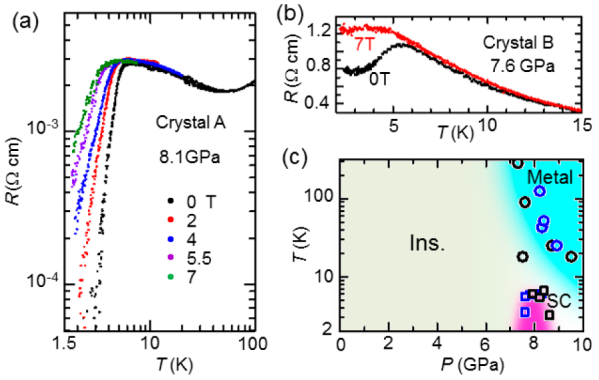

Figure 4. (a) The resistivity behavior under magnetic field (crystal A, 0−7 T). (b) Another example of the magnetic field dependence of the low-temperature resistivity behavior (crystal B). (c) P−T phase diagram. Open circles are T_{min} where the temperature dependence of the resistivity took a resistivity minimum. Open squares are the onset temperature of superconducting transition.

drop was suppressed by applying a magnetic field. Similar measurements were also made for other crystals (crystal B (Figure 4b) and crystal D (see SI)). A small resistivity drop at 7.6 GPa and the almost complete suppression of this resistivity drop at 7 T (Figure 4b) indicated that the lowest pressure of the superconducting region in the pressure−temperature (P−T) phase diagram was ~7.5 GPa. The P−T phase diagram is presented in Figure 4c. The superconducting phase appeared in the pressure range of 7.5−8.6 GPa at T > 3.3 K. Similar to representative organic superconductors with 2D electronic structures, such as κ-ET_2X,[12a] the superconducting phase of [Ni(hfdt)$_2$] appeared just above the critical pressure where the semiconducting phase was suppressed by pressure.[11,12b]

To understand the origin of pressure dependence of the conductivity, we performed first-principle electronic-structure calculations as a function of pressure (Figure 5). Starting from

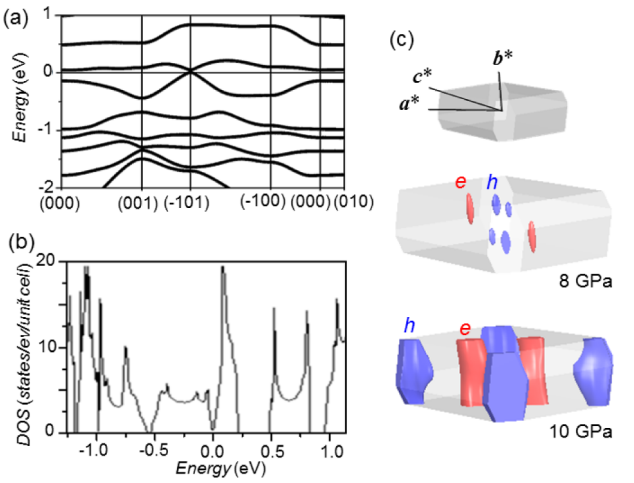

Figure 5. (a) Electronic band energy dispersion at 8 GPa. k-points are described in units of (a*/2,b*/2,c*/2). (b) Electronic density of states at 8 GPa. (c) Electron and hole Fermi surfaces at 8 and 10 GPa.

the experimental structure at ambient pressure and 200 K, the lattice parameters and atomic positions are computationally optimized applying a hydrostatic pressure of 6−11 GPa. We used our computational code QMAS (Quantum MAterials Simulator)[28] based on the projector augmented-wave method[29] with the generalized gradient approximation (GGA)[30] to describe exchange-correlation energy. The obtained lattice parameters are plotted in Figure 2c. They decrease monotonously with pressure increasing. The compressibility of the a axis is slightly smaller than those of the other axes.

The calculated band gap at ambient pressure (~0.12 eV) is significantly smaller than the value expected from the activation energy (E_a) of the resistivity (~0.14 eV) (see also Figure 3c).[24] This is general tendency of the GGA (and the local density approximation also). At 6 GPa, the band gap is calculated to be 0.01 eV, and at 8 GPa, the band gap disappears and the system becomes a semimetal with Fermi surfaces consisting of small hole and electron pockets as shown in Figure 5. This pressure variation of the band gap is consistent with the variation of the activation energy shown in Figure 3c. The sizes of Fermi surfaces grow with pressure. At 10 GPa, there are quasi-2D hole and electron Fermi surfaces as shown in Figure 5c. To clarify, the relationship between the experimentally observed superconductivity and the calculated electronic structures is a future issue.

In summary, the four-probe resistivity measurements were performed on the single-component molecular conductor, [Ni(hfdt)$_2$] up to 10 GPa by using DAC technique. The resistivity decreased with pressure, and the activation energy became zero at around 7.5 GPa. The superconducting transition was observed at 7.5−8.6 GPa. Such resistivity behavior was reproduced by the first-principle crystal and electronic band structure calculations, which indicates the superconducting phase of [Ni(hfdt)$_2$] appears just after the low-temperature insulating phase is suppressed by pressure.

dx.doi.org/10.1021/ja503690m | J. Am. Chem. Soc. 2014, 136, 7619−7622

■ ASSOCIATED CONTENT

Supporting Information

Experimental detials and data. This material is available free of charge via the Internet at http://pubs.acs.org.

■ AUTHOR INFORMATION

Corresponding Author

hayao@chs.nihon-u.ac.jp; akoba@chs.nihon-u.ac.jp

Notes

The authors declare no competing financial interest.

■ ACKNOWLEDGMENTS

H.K. and A.K. thank B. Zhou, Y. Idobata, and M. Nakamura for their help in low-temperature structural studies and EPMA experiments. This work was financially supported by the "Strategic Research Base Development" Program for Private Universities subsidized by MEXT (2009) (S0901022) and Grant-in-Aid for Scientific Research (S) (no. 22224006) from the Japan Society for the Promotion of Science (JSPS).

■ REFERENCES

(1) Jerome, D.; Mazaud, A.; Ribault, M.; Bechgaard, K. *J. Phys., Lett.* **1980**, *41*, L95.

(2) Brossard, L.; Bousseau, M.; Ribault, M.; Valade, L.; Cassoux, P. *C. R. Acad. Sci. Paris* **1986**, *302*, 205.

(3) Kobayashi, A.; Fujiwara, E.; Kobayashi, H. *Chem. Rev.* **2004**, *104*, 5243.

(4) Kobayashi, A.; Tanaka, H.; Kobayashi, H. *J. Mater. Chem.* **2001**, *11*, 2078.

(5) (a) Yokota, T.; Takeshita, N.; Shimizu, K.; Amaya, K.; Onodera, A.; Shirotani, I.; Endo, S. *Czech. J. Phys.* **1996**, *46* (Suppl.S2), 817. (b) Iwasaki, E.; Shimizu, K.; Amaya, K.; Nakayama, A.; Aoki, K.; Calon, R. P. *Synth. Met.* **2001**, *120*, 1003.

(6) (a) Narvor, L. N.; Robertson, N.; Weyland, T.; Kilburn, J. D.; Underhill, A. E.; Webster, M.; Svenstrup, N.; Becher, J. *Chem. Commun.* **1996**, 1363. (b) Schiødt, N. C.; Bjørnholm, T.; Bechgaard, K.; Neumeier, J. J.; Allgeier, C.; Jacobsen, C. S.; Thorup, C. S. *Phys. Rev.* **1996**, *B53*, 1773.

(7) Tanaka, H.; Okano, Y.; Kobayashi, H.; Suzuki, W.; Kobayashi, A. *Science* **2001**, *291*, 285.

(8) Belo, D.; Alves, H.; Lopes, E. B.; Duarte, M. T.; Gama, V.; Henriques, R. T.; Almeida, M.; Perez-Benltez, A.; Rovira, C.; Veciana, J. *Chem.—Eur. J.* **2001**, *7*, 511.

(9) Rovira, C.; Novoa, J. J.; Mozos, J.-L.; Ordejon, P.; Canadell, E. *Phys. Rev.* **2002**, *B65*, 081104(R).

(10) Tanaka, H.; Tokumoto, M.; Ishibashi, S.; Graf, D.; Choi, E. S.; Brooks, J. S.; Yasuzuka, S.; Okano, Y.; Kobayashi, H.; Kobayashi, A. *J. Am. Chem. Soc.* **2004**, *126*, 10518.

(11) Seo, H.; Hotta, C.; Fukuyama, H. *Chem. Rev.* **2004**, *104*, 5005.

(12) (a) Williams, J. M.; Ferraro, J. R.; Thorn, R. J.; Carlson, K. D.; Geiser, U.; Wang, H. H.; Kini, A. M.; Wangbo, M.-H. *Organic Superconductors (Including Fillerenes): Synthesis, Structure, Properties and Theory*; Prentice Hall: NJ, 1992. (b) Miyagawa, K.; Kanoda, K.; Kawamoto, A. *Chem. Rev.* **2004**, *104*, 5635.

(13) (a) Suzuki, W.; Fujiwara, E.; Kobayashi, A.; Fujishiro, Y.; Nishibori, E.; Takata, M.; Sakata, M.; Fujiwara, H.; Kobayashi, H. *J. Am. Chem. Soc.* **2003**, *125*, 1486. (b) Zhou, B.; Shimamura, M.; Fujiwara, E.; Kobayashi, A.; Higashi, T.; Nishibori, E.; Sakata, M.; Cui, H.; Takahashi, K.; Kobayashi, H. *J. Am. Chem. Soc.* **2006**, *128*, 3872.

(14) Zhou, B.; Idobata, Y.; Kobayashi, A.; Cui, H.-B.; Kato, R.; Takagi, R.; Miyagawa, K.; Kanoda, K. *J. Am. Chem. Soc.* **2012**, *134*, 12724.

(15) Zhou, B.; Kobayashi, A.; Okano, Y.; Nakashima, T.; Aoyagi, S.; Nishibori, E.; Sakata, M.; Tokumoto, M.; Kobayashi, H. *Adv. Mater.* **2009**, *21*, 3596.

(16) Ishibashi, S.; Tanaka, H.; Kohyama, M.; Tokumoto, M.; Kobayashi, A.; Kobayashi, H.; Terakura, K. *J. Phys. Soc. Jpn.* **2005**, *74*, 843.

(17) Ishibashi, S.; Terakura, K.; Kobayashi, A. *J. Phys. Soc. Jpn.* **2008**, *77*, 024702.

(18) Seo, H.; Ishibashi, S.; Okano, Y.; Kobayashi, H.; Kobayashi, A.; Fukuyama, H.; Terakura, K. *J. Phys. Soc. Jpn.* **2008**, *77*, 023714.

(19) Seo, H.; Ishibashi, S.; Otsuka, Y.; Fukuyama, H.; Terakura, K. *J. Phys. Soc. Jpn.* **2013**, *82*, 054711.

(20) Kobayashi, A.; Tanaka, H.; Kumasaki, M.; Torii, H.; Narymbetov, B.; Adachi, T. *J. Am. Chem. Soc.* **1999**, *121*, 10763.

(21) Cui, H.-B.; Brooks, J. S.; Kobayashi, A.; Kobayashi, H. *J. Am. Chem. Soc.* **2009**, *131*, 6358.

(22) (a) Tenn, N.; Bellec, N.; Jeannin, O.; Piekara-Sady, L.; Auban-Senzier, P.; Iniguez, J.; Canadell, E.; Lorcy, D. *J. Am. Chem. Soc.* **2009**, *131*, 16961. (b) Yzambart, G.; Bellec, N.; Nasser, G.; Jeannin, O.; Roisnel, T.; Fourmigue, M.; Auban-Senzier, P.; Iniguez, J.; Canadell, E.; Lorcy, D. *J. Am. Chem. Soc.* **2012**, *134*, 17138. (c) Cui, H.; Tsumuraya, T.; Miyazaki, T.; Y. Okano, Y.; Kato, R. *Eur. J. Inorg. Chem.*, DOI:10.1002/ejic.20140013.

(23) Tse, J. S.; Leitch, A. A.; Yu, X.; Bao, X.; Zhang, S.; Liu, Q.; Jin, C.; Secco, A.; Desgreniers, S.; Ohishi, Y.; Oakley, R. T. *J. Am. Chem. Soc.* **2010**, *132*, 4876. (b) Leitch, A. A.; Lekin, K.; Winter, S. M.; Downie, L.; Tsuruda, H.; Tse, J. S.; Mito, M.; Desgreniers, S.; Dube, P. A.; Zhang, S.; Liu, Q.; Jin, C.; Ohishi, Y.; Oakley, R. T. *J. Am. Chem. Soc.* **2011**, *133*, 6051.

(24) Sasa, M.; Fujiwara, E.; Kobayashi, A.; Ishibashi, S.; Terakura, K.; Okano, Y.; Fujiwara, H.; Kobayashi, H. *J. Mater. Chem.* **2005**, *15*, 155.

(25) Rivera, N. M.; Engler, E. M.; Schumaker, R. R. *J. Chem. Soc. Chem. Commun.* **1979**, 184.

(26) Dautel, O. J.; Fourmigue, M. *Inorg. Chem.* **2001**, *40*, 2083.

(27) Zhou, B.; Yajima, H.; Idobata, Y.; Kobayashi, A.; Kobayashi, T.; Nishibori, E.; Sawa, H.; Kobayashi, H. *Chem. Lett.* **2012**, *41*, 154.

(28) *Quantum MAterials Simulator*; http://qmas.jp, accessed Oct 14, 2013.

(29) Blöchl, P. E. *Phys. Rev. B* **1994**, *50*, 17953.

(30) Perdew, J. P.; Burke, K.; Ernzerhof, M. *Phys. Rev. Lett.* **1996**, *77*, 3865.